

Photodissociation dynamics of O_3^- at 523 nm

M.C. Garner, C.R. Sherwood, K.A. Hanold, R.E. Continetti

Department of Chemistry and Biochemistry, University of California, San Diego, 9500 Gilman Drive, La Jolla, CA 92093-0314, USA

Received 28 August 1995; in final form 20 October 1995

Abstract

The photodissociation dynamics of O_3^- at 523 nm have been studied using fast-ion-beam translational energy spectroscopy. Translational energy and angular distributions of coincident $O^- + O_2$ products from the process $O_3^- + h\nu \rightarrow O^- + O_2$ were measured. O_3^- was generated by electron-impact in a pulsed beam from two precursors – neat O_2 and a seeded beam of O_3 . The observed photodissociation dynamics are very different in the two cases, indicating a great difference in internal excitation of ozonide in the two sources.

1. Introduction

The ozonide anion (O_3^-) has been identified as an important negative ion in the chemistry of the D region of the ionosphere [1]. The primary photochemical processes and photodissociation dynamics of this anion are thus of interest as a greater understanding of the dynamics of the ionosphere is gained. O_3^- is known to undergo both photodetachment and photodissociation from the visible into the ultraviolet region of the spectrum. Photoelectron spectroscopy [2,3] of O_3^- and low-energy electron scattering from O_3 [4] have also been used to study the poorly characterized low-lying triplet states of O_3 . To further clarify the roles played by photodissociation and photodetachment in this system, we have initiated experiments on the photodestruction dynamics of O_3^- . The work reported here concerns the ionic photodissociation of O_3^- at 523 nm. These experiments reveal very different dissociation dynamics from two sources of O_3^- .

The gas-phase photochemistry of O_3^- has been the subject of a variety of experimental studies, including photodestruction cross-sections [2,5–8],

photodissociation [9,10] and photodetachment [2,11–13] cross sections, and studies of the photoelectron spectra at selected wavelengths [2,3]. In addition, there have been several investigations of the reactions of O_3^- with various species of atmospheric interest [14,15]. Collision-induced dissociation studies have also been carried out to study the energetics of this species [16]. There has been no study of the detailed photodissociation dynamics of O_3^- to date.

Photodestruction cross section measurements by Lineberger and co-workers reveal that excitation of O_3^- at ≈ 523 nm results primarily in photodissociation, with a photodetachment cross section ≈ 15 times lower [2]. Vibrational structure is found in all of the photochemical cross sections measured for O_3^- in the 520 nm range. This has been attributed to symmetric stretch and bending progressions in a predissociated excited state of O_3^- [7]. Hiller and Vestal made an indirect measurement of the product angular distribution in the visible photodissociation of O_3^- , and concluded that a parallel electronic transition from the ground state of O_3^- , $\tilde{A}(^2A_2) \leftarrow \tilde{X}(^2B_1)$, is responsible for dissociation into $O^- + O_2$ at 523 nm [10]. Below 500 nm, Hiller and Vestal

observed the $O + O_2^-$ channel and a more isotropic angular distribution, which they ascribed to involvement of the $\tilde{B}(^2A_1)$ excited state. The observed threshold for the $O + O_2^-$ channel led Hiller and Vestal to assign an $O^- - O_2$ bond energy $D_0 \leq 1.39$ eV. This value is at variance with the bond energy of $D_0 = 1.69$ eV obtained from the $O - O_2$ bond energy of O_3 ($D_0 = 1.05$ eV) [17], the electron affinity of O_3 (EA = 2.103 eV) [3], and the electron affinity of O (EA = 1.46 eV) [18]. While this discrepancy may result from vibrational hot bands in O_3^- , it is also possible that a long-lived excited state or isomeric form of O_3^- may be formed in the ion source. In addition, evidence for an excited state of $O_3^- \approx 0.4$ – 0.8 eV above the ground state has been observed in collision-induced dissociation experiments by Lifshitz et al. [15,16].

There has been considerably less theoretical work done on O_3^- . Configuration interaction (CI) calculations were carried out on O_3 and O_3^- to determine the electron affinity by Kaufman and co-workers over 20 years ago [19]. Peterson et al. [20] have determined vibrational frequencies of the ground 2B_1 state and geometries for the first three excited electronic states of O_3^- . Koch et al. [21] carried out multi-reference CI calculations on the three lowest lying doublet states of O_3^- , to compare to matrix absorption studies of KO_3 and RbO_3 [22]. The most recent study by Borowski et al. [23] has provided a high-level prediction of the geometry, vibrational frequencies and infrared intensities for the ground state of O_3^- . The calculations to date have chiefly considered C_{2v} geometries near that for the ground state of O_3 , with no calculations for cyclic conformers of O_3^- . Cyclic states of O_3 have received considerable attention, however [24]. No predictions of quartet states of O_3^- have been made to date.

In this Letter, we report a study of the photodissociation dynamics of O_3^- at 523 nm. By using two different sources of O_3^- , we have observed a large change in the photodissociation dynamics. Production of O_3^- by electron-impact on O_2 yields photodissociation spectra with resolved O_2 vibrational structure, and photofragment kinetic energy releases consistent with the established thermochemistry of the ground state of O_3^- . Production of O_3^- by electron-impact on O_3 yields photodissociation spectra with no resolved structure and a 0.35 eV larger

kinetic energy release. The great difference in the dissociation dynamics for these two different sources of O_3^- may be due to either rovibrational excitation of O_3^- or a low-lying electronic state with a different geometry.

2. Experimental

These experiments rely on translational energy spectroscopy of molecular photofragments. A fast beam of mass-selected anions is intersected with the output of a pulsed laser and the resulting photofragments are detected by a two-particle time-and-position sensitive detector. The spectrometer is configured to detect both atomic or molecular fragments from a single binary dissociation *in coincidence*. A schematic view of the experimental geometry is shown in Fig. 1. Given the parent ion mass and velocity, measurement of the time and position of arrival of the photofragments provides the information necessary to determine the mass, energy and recoil angle of the products on an event-by-event basis [25,26]. A brief description of the apparatus has been published [27,28], and a brief review is supplied here.

The design of the ion-beam line is similar to that used by Neumark and co-workers to study free-radical photodissociation [29]. O_3^- is produced and cooled by electron-impact in a pulsed free-jet expansion intersected by a 1 keV electron beam [29]. The anions pass through a skimmer into a differentially pumped chamber, are accelerated to kinetic energies of 2.5–4 keV, and mass-selected by time-of-flight.

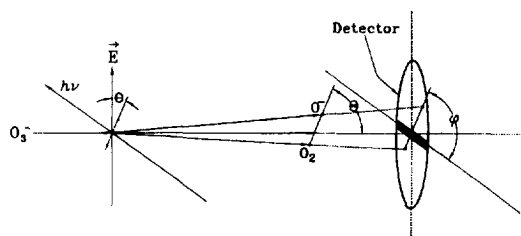


Fig. 1. Schematic of the experimental geometry, indicating center-of-mass recoil angle Θ and the recoil angle relative to the electric vector (shown in the vertical polarization) θ . Time and position of arrival for both O^- and O_2 photofragments are recorded by the detector.

O_3^- anions are intersected by the linearly polarized 523 nm output of a Nd:YLF laser (Spectra Physics TFR). The laser pulse is 6 ns full-width-at-half-maximum with an energy of 200 μJ /pulse at 523 nm and is focused to a spot of ≈ 0.5 mm diameter. These experiments were performed at apparatus repetition rates of 300–500 Hz. Photoelectron spectra may also be measured by straight time-of-flight using a second time- and position-sensitive detector [30].

Photofragments recoil out of the beam over a 96 cm flight path between the laser interaction region and the particle detector. Photofragments that clear a 7 mm wide beam-block strip, centered on the ion beam, strike a 40 mm diameter field-of-view microchannel-plate particle detector. This detector uses two side-by-side wedge-and-strip anodes [29] to record the time and position of arrival of fragments. The detector face is at ground potential, allowing both neutral and ionic products to be detected. Detector calibration was performed by recording data on the photodissociation of O_2^- at 262 nm [31], yielding an energy resolution $\Delta E/E \approx 10\%$ at 0.62 eV.

There are two possible modes of data acquisition – collection of only neutral *or* neutral and ionic photofragments. Electrostatic deflection of ions out of the beam after the laser interaction region allows detection of only neutral photofragments. If no deflection field is used, both ionic and neutral photofragments are detected. These modes allow us to distinguish ion photodissociation processes ($O_3^- + h\nu \rightarrow O^- + O_2$ or $O + O_2^-$) from dissociative photodetachment ($O_3^- + h\nu \rightarrow O + O_2 + e^-$). The dissociation dynamics data presented consists of only pairs of *coincident* fragments (ions + neutrals) originating from a single dissociation event as determined by the conservation of linear momentum in the center-of-mass frame. Detection of the fragments in coincidence allows determination of the product masses, translational energy release and center-of-mass recoil angle for each dissociation event [25,29].

Examination of spectra recorded with the ion deflector on indicated that only $O^- + O_2$ fragments were produced in these experiments. Photoelectron spectra at 523 nm revealed only photodetachment of nascent O^- by a second photon following photodissociation. The absence of O_2^- photodetachment confirms the absence of the $O + O_2^-$ dissociation channel at 523 nm. Measurements of the translational

energy release at 2.5 and 4 keV beam energies were consistent, indicating that dissociation of O_3^- occurs fast relative to the 7.5 μs center-of-mass flight time from the laser interaction region to the detector at 4 keV.

Two methods were used to generate O_3^- : electron-impact on a neat expansion of O_2 (O_3^-/O_2) and electron-impact on dilute O_3 seeded in 30% He/70% Ne (O_3^-/O_3). O_3 was synthesized from high-purity O_2 in a commercial ozonator and adsorbed on silica gel at -78°C . Production of the excited state of O_3^- by electron impact on O_3 requires that any residual O_2 be assiduously removed by pumping on the silica-adsorbed O_3 .

Center-of-mass (c.m.) translational energy and angular distributions are extracted from the raw data by numerically correcting for the finite angular acceptance of the detector. The anisotropy of the angular distribution as a function of translational energy release (E_T) is found by separating the doubly differential cross section $P(E_T, \theta)$ into energy and angular distributions as $P(E_T, \theta) = P(E_T)[1 + \beta(E_T)P_2(\cos \theta)]$ [29]. In this equation, $P_2(\cos \theta)$ is the second Legendre polynomial in $\cos \theta$ and θ is the angle between the CM recoil velocity and the electric vector of the laser beam [32]. Using this expression, $\beta = 2$ corresponds to a pure ‘parallel’ transition, with a $\cos^2\theta$ angular distribution and $\beta = -1$ corresponds to a pure ‘perpendicular’ transition, with a $\sin^2\theta$ angular distribution [32]. The distributions $P(E_T)$ and $\beta(E_T)$ are then found by a least-squares fit. The weights for the data as a function of E_T and θ are calculated from the finite laboratory angular acceptance of the detector [29].

3. Results

Kinetic-energy-release (KER) spectra for the photodissociation of O_3^- are shown in Fig. 2. These spectra are the raw data, with no correction made for the limited angular acceptance of the detector. The top frame shows KER spectra for O_3^-/O_2 . These spectra show structure consistent with resolved vibrational excitation of the O_2 fragment, and show an upper limit to the KER of ≈ 0.75 eV. The two spectra shown in this frame are for horizontal and vertical polarization of the photodissociation laser

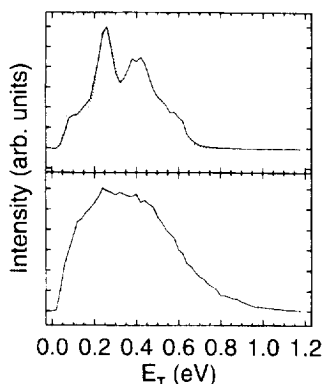


Fig. 2. Raw kinetic energy release spectra recorded for coincident O^- and O_2 photofragments. Top frame: spectra recorded from O_3^-/O_2 at a beam energy of 2.5 keV. Solid line data recorded with horizontal laser polarization, dashed line with vertical polarization. Bottom frame: spectra recorded from O_3^-/O_3 at a beam energy of 2.5 keV with horizontal laser polarization.

relative to the ion beam. The vertical polarization spectrum in particular reveals the presence of a low KER peak consistent with the formation of $O_2(v=3)$. The KER spectrum for O_3^-/O_3 is shown in the lower frame. This spectrum, recorded with horizontal laser polarization, is smooth and extends to significantly higher kinetic energy releases (1.1 eV).

The center-of-mass translational energy and angular distributions obtained after correction for the finite angular acceptance of the detector are shown in Figs. 3 and 4 for O_3^-/O_2 and O_3^-/O_3 , respectively. The translational energy distributions are shown as $P(E_T)$, while the dependence of the angular distributions on translational energy release are shown as the energy dependence of the anisotropy parameter, $\beta(E_T)$. The $P(E_T)$ and $\beta(E_T)$ curves are both averaged over 0.020 eV energy bins, with the exception of $\beta(E_T)$ for O_3^-/O_3 which is averaged over 0.060 eV bins.

In the case of O_3^-/O_2 , the $P(E_T)$ confirms the observation in the raw data of a vibrationally resolved KER spectrum. The upper limit to the $P(E_T) \approx 0.75$ eV is consistent with the known energetics of the ground state of O_3^- . The effect of the energy and angular dependence of the detector acceptance is seen in the accentuation of signal at low E_T . No events are detectable with $E_T < 0.065$ eV given the experimental geometry. The $P(E_T)$ suggests a vibra-

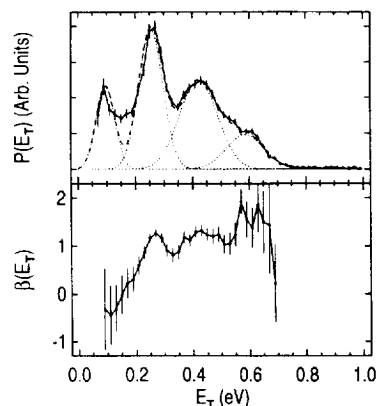


Fig. 3. Top frame: center-of-mass translational energy distribution $P(E_T)$ for O_3^-/O_2 shown as a solid line and points with error bars ($\pm 2\sigma$) from the least squares fit. Decomposition of $P(E_T)$ into Gaussian peaks representing $O_2(v=0, 1, 2$ and $3)$ is shown by the short-dashed lines, with the long-dashed line giving the sum of the Gaussians. Bottom frame: Anisotropy parameter β as a function of E_T for O_3^-/O_2 shown as points with error bars ($\pm 2\sigma$) and solid line.

tional inversion in the O_2 photofragments with a decrease in rotational excitation as vibrational excitation increases. In Fig. 3, an attempt is made to quantify this by fitting four Gaussian functions to the $P(E_T)$. The (approximate) state distribution extracted in this manner is: $v=0$: 14%, $v=1$: 35%, $v=2$: 35%, $v=3$: 16%. The $\beta(E_T)$ curve in this

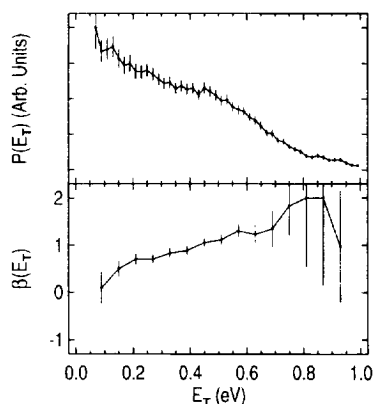


Fig. 4. Top frame: Center-of-mass translational energy distribution $P(E_T)$ for O_3^-/O_3 shown as points with error bars ($\pm 2\sigma$) and solid line. Bottom frame: Anisotropy parameter β as a function of E_T for O_3^-/O_3 shown as points with error bars ($\pm 2\sigma$) and solid line.

case indicates a parallel ($\langle \beta \rangle = 1.11 \pm 0.05$) dissociative transition, with a clear trend for more positive values at higher E_T . It is also of interest to note the corresponding peaks in the $P(E_T)$ and $\beta(E_T)$ at 0.27 eV, corresponding to production of $O_2(\nu = 2)$.

The $P(E_T)$ curve for O_3^-/O_3 shows no structure, with a monotonic increase towards lower E_T . This increase is once again an effect of the limited detector acceptance at low E_T . The immediate implication of the change in the $P(E_T)$ from O_3^-/O_2 is that the propensity towards high vibrational–low rotational excitation in the O_2 fragment is significantly reduced. The $\beta(E_T)$ curve for O_3^-/O_3 also indicates a parallel ($\langle \beta \rangle = 0.93 \pm 0.05$) dissociative transition, with the trend for more positive values at higher E_T . No structure is evident in the $\beta(E_T)$ curve.

4. Discussion

4.1. O_3^-/O_2

These results are consistent with earlier work [2,7,10] which has shown that the photodissociation $O_3^- \rightarrow O_2(^3\Sigma_g^-) + O^-$ is the dominant photodissociation pathway in this wavelength region. Observation of a parallel transition is consistent with earlier studies [10] which indicated that excitation from the ground 2B_1 state to the 2A_2 state is responsible for photodissociation at 523 nm. As noted in Section 3, the maximum $E_T \approx 0.75$ eV is consistent with the energetics of the ground state of O_3^- , as determined by the electron affinities of O_3 , O and the bond energy O– O_2 , if we assume that 0.06 eV internal energy in O_3^- appears in translational of the photofragments.

The apparent narrowing of the product rotational distribution with increasing O_2 vibrational excitation is of interest. This effect may simply be a result of angular momentum conservation, since the orbital angular momentum of the fragments is constrained at low translational energy releases. A classical impulse model qualitatively predicts the observed distribution. Dissociation of linear O_3 configurations would be expected to produce more vibrational excitation in the O_2 fragment and less torque on the O_2 product, reducing the orbital angular momentum which must be balanced by rotational excitation of the O_2 . The

actual mechanism, which appears to involve predissociation of the \tilde{A} state of O_3^- , may be considerably more complicated.

The large average value of $\langle \beta \rangle \approx 1.1$ indicates that predissociation of the excited state of O_3^- is occurring on the time scale of a rotational period over the range of E_T . The overall energy dependence of $\beta(E_T)$ suggests that an inverse correlation exists between the lifetime of the predissociating state and the product translational energy release. The peak in $\beta(E_T)$ at 0.27 eV, assigned in the $P(E_T)$ to the production of $O_2(\nu = 2)$, may imply a mode-dependent lifetime in the predissociation of O_3^- . Asymmetric stretch excitation of the ground state of O_3^- has been observed by Neumark and co-workers [3] in the production of O_3^- by electron impact on O_2 . This excitation would be expected to carry over into the excited state through sequence bands. Hiller and Vestal [10], following calculations by Pack [33] assumed that the reaction coordinate for dissociation of the $\tilde{A}(^2A_2)$ state excited at 523 nm is along the asymmetric stretch coordinate with no barrier in the exit channel. Recent theoretical calculations by Peterson et al. [20] have confirmed the repulsive nature of the asymmetric stretch coordinate for this state. Thus, it is possible that asymmetric stretch excitation of O_3^- will play an important role in promoting both the rapid dissociation of O_3^- and the production of vibrationally excited O_2 products. If asymmetric stretch excitation adiabatically correlates to vibrationally excited O_2 , however, this energy will not appear in translation and interpretation of the observed $P(E_T)$ becomes more difficult.

An alternative mechanism, presented by Lineberger and co-workers [2], suggested that dissociation may proceed by elimination of the central O atom as O^- . A mechanism of this type would also be expected to produce significant vibrational excitation in the O_2 products, as we have observed. The observed parallel angular distribution, however, argues against this mechanism. The transition moment for the $^2A_2 \leftarrow ^2B_1$ transition lies in the O–O–O plane, along the y axis in C_{2v} symmetry [34]. Thus, a parallel electronic transition followed by rapid elimination of the central atom as O^- might be expected to result in the O^- and O_2 products recoiling *perpendicular* to the transition moment, yielding a negative anisotropy parameter.

4.2. O_3^- / O_3

In the case of O_3^- produced by electron-impact on O_3 the photodissociation dynamics are very different. The broad, featureless KER spectrum suggests that in this case photodissociation produces little vibrational excitation of O_2 and large rotational excitation. In addition, the 0.35 eV higher kinetic energy release observed must either come from internal excitation in the ground state of O_3^- or a new (isomeric) electronic state of O_3^- . While it is possible that the O_3^- / O_3 source produces much greater rotational and vibrational excitation than O_3^- / O_2 , in photoelectron spectroscopy measurements Neumark and co-workers find *less* vibrational excitation from O_3^- / O_3 than O_3^- / O_2 in an electron-impact source similar to that used in this work [3]. In addition, recent photodissociation cross-section studies by Ray and co-workers have been interpreted in terms of an excited state of O_3^- , with no evidence observed in the photoelectron spectrum [35]. To rule out parent O_3^- rotational and vibrational excitation as the cause of the extremely different photodissociation dynamics observed for O_3^- / O_3 , further photoelectron spectroscopy experiments will be required.

A second explanation for the observed dynamics is that an excited state, O_3^{*-} , of a significantly different geometry, is formed by ion-molecule reactions in the O_3^- / O_3 source. As noted in Section 1, there have been significant discrepancies between previous determinations of the energetics of O_3^- . Hiller and Vestal [10], in their study of the threshold for the $O + O_2^-$ dissociation channel, found evidence for a state with an $O^- - O_2$ bond energy of < 1.39 eV. If 1.1 eV is taken as the maximum E_T in the current experiments, and if we assume that ground state fragments are produced, an $O^- - O_2$ bond energy of 1.27 eV is indicated. Collision-induced dissociation (CID) experiments on O_3^- formed from O_3 / H_2O mixtures found evidence for an excited ionic state ≈ 0.84 eV above the ground state of O_3^- [15,16]. The CID experiments on O_3^- formed from $O_3 / H_2O / N_2O$ mixtures showed an intermediate excitation of ≈ 0.40 eV above the ground state of O_3^- [15,16]. This latter energy is qualitatively consistent with the present results and those of Hiller and Vestal. In none of these experiments can rotational and vibrational excitation of the parent be unambigu-

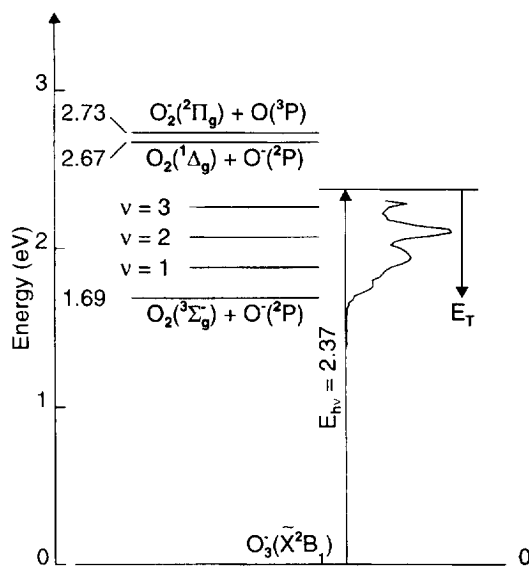


Fig. 5. Energetics diagram for the photodissociation of the ground state of O_3^- , showing the possible low-lying product channels. The $P(E_T)$ for O_3^- / O_2 is shown superimposed on the internal energy scale.

ously separated from electronic energy. However, it is certainly possible that an isomeric form of O_3^- is present. The results of the current experiment, be they due to rovibrational or electronic excitation of the parent O_3^- , help explain some of the discrepancies observed in earlier studies of O_3^- discussed in Section 1.

The energetics of the photodissociation of the ground state of O_3^- are illustrated in Fig. 5. If an excited state, O_3^{*-} , is involved, the present experiments cannot unambiguously determine the relative energy of this state. If we assume that the products of the photodissociation are ground state $O^-(^2P)$ and $O_2(^3\Sigma_g^-)$, O_3^{*-} would be ≈ 0.42 eV above the ground state of O_3^- . If the products of the photodissociation are $O^-(^2P) + O_2(^1\Delta_g)$, O_3^{*-} would be ≈ 1.57 eV above the ground state of O_3^- . Peterson et al. [20] have found evidence for a bound 2B_2 state of O_3^- 1.30 eV above the ground state of O_3^- in C_{2v} symmetry. The inferred high rotational excitation and low vibrational excitation in the O_2 photofragments from O_3^{*-} implies that the geometry of this possible excited state may be extremely bent or even cyclic. Theoretical guidance concerning both highly bent states and possible quartet states of O_3^- may provide insights into the nature of O_3^{*-} .

5. Conclusions

In this Letter, we report the first study of the photodissociation dynamics of O_3^- using fast-ion-beam photofragment translational spectroscopy. A striking change in the photodissociation dynamics is observed from two sources of O_3^- . Production of O_3^- by electron impact on O_2 yields a vibrationally resolved kinetic energy release channel for the $O^- + O_2$ photodissociation channel. Production of O_3^- by electron impact on O_3 , on the other hand, produces an $O^- + O_2$ photodissociation channel with no resolvable vibrational excitation and 0.35 eV larger maximum kinetic energy release. The implications of these results for the photodissociation of both the ground state of O_3^- and a possible excited state of O_3^-* are discussed. A measurement of the photoelectron spectrum of O_3^-* is currently underway to aid in the determination of whether this phenomenon is due to vibrational and rotational excitation of O_3^- , or an electronically excited state. Further experimental studies of O_3^- photodissociation at other wavelengths, along with theoretical guidance, are ultimately needed to better understand the photodissociation dynamics of this simple negative ion.

Acknowledgement

This work was supported by the National Science Foundation. REC gratefully acknowledges further support from the Camille and Henry Dreyfus Foundation (New Faculty Award) and the David and Lucile Packard Foundation (1994 Fellowship in Science and Engineering). REC acknowledges helpful discussions with Dr. D. Ray and Dr. D.W. Arnold.

References

- [1] H.S.W. Massey, in: Applied atomic collision physics, Vol. 1. Atmospheric physics and chemistry, ed. H.S.W. Massey (Academic Press, New York, 1982) pp. 126–130.
- [2] S.E. Novick, P.A. Engelking, P.L. Jones, J.H. Futrell and W.C. Lineberger, *J. Chem. Phys.* 70 (1979) 2652.
- [3] D.W. Arnold, C. Xu, E.H. Kim and D.M. Neumark, *J. Chem. Phys.* 101 (1994) 912.
- [4] N. Swanson and R.J. Celotta, *Phys. Rev. Letters* 35 (1975) 783.
- [5] J.R. Peterson, *J. Geophys. Res.* 81 (1976) 1433.
- [6] P.C. Cosby, J.H. Ling, J.R. Peterson and J.T. Moseley, *J. Chem. Phys.* 65 (1976) 5267.
- [7] P.C. Cosby, J.T. Moseley, J.R. Peterson and J.H. Ling, *J. Chem. Phys.* 69 (1978) 2771.
- [8] G.P. Smith and L.C. Lee, *J. Chem. Phys.* 71 (1979) 2323.
- [9] M.L. Vestal and G.H. Mauclaire, *J. Chem. Phys.* 67 (1977) 3767.
- [10] J.F. Hiller and M.L. Vestal, *J. Chem. Phys.* 74 (1981) 6096.
- [11] R. Byerly Jr. and E.C. Beatty, *J. Geophys. Res.* 76 (1971) 4596.
- [12] S.F. Wong, T.V. Vorburger and S.B. Woo, *Phys. Rev. A* 5 (1972) 2598.
- [13] L.J. Wang, S.B. Woo and E.M. Helmy, *Phys. Rev. A* 35 (1987) 759.
- [14] I. Dotan, J.A. Davidson, G.E. Streit, D.L. Albritton and F.C. Fehsenfeld, *J. Chem. Phys.* 67 (1977) 2874.
- [15] C. Lifshitz, R.L.C. Wu, T.O. Tiernan and D.T. Terwilliger, *J. Chem. Phys.* 68 (1978) 247.
- [16] R.L.C. Wu, T.O. Tiernan and C. Lifshitz, *Chem. Phys. Letters* 51 (1977) 211.
- [17] J.L. Gole and R.N. Zare, *J. Chem. Phys.* 57 (1972) 5331.
- [18] D.M. Neumark, K.R. Lykke, T. Anderson and W.C. Lineberger, *Phys. Rev. A* 32 (1985) 1890.
- [19] M.M. Heaton, A. Pipano and J.J. Kaufman, *Intern. J. Quantum Chem.* 6 (1972) 181.
- [20] K.A. Peterson, R.C. Mayrhofer and R.C. Woods, *J. Chem. Phys.* 93 (1990) 5020.
- [21] W. Koch, G. Frenking, G. Steffen, D. Reinen, M. Jansen and W. Assenmacher, *J. Chem. Phys.* 99 (1993) 1271.
- [22] G. Steffen, W. Hesse, M. Jansen and D. Reinen, *Inorg. Chem.* 30 (1991) 1923.
- [23] P. Borowski, B.O. Roos, S.C. Racine, T.J. Lee and S. Carter, *J. Chem. Phys.* 103 (1995) 266.
- [24] A. Banichevich, S.D. Peyerimhoff and F. Grein, *Chem. Phys.* 178 (1993) 155, and references therein.
- [25] D.P. DeBruijn and J. Los, *Rev. Sci. Instrum.* 53 (1982) 1020.
- [26] R.E. Continetti, D.R. Cyr, D.L. Osborn, D.J. Leahy and D.M. Neumark, *J. Chem. Phys.* 99 (1993) 2616.
- [27] C.R. Sherwood, M.C. Garner, K.A. Hanold, K.M. Strong and R.E. Continetti, *J. Chem. Phys.* 102 (1995) 6949.
- [28] R.E. Continetti, C.R. Sherwood, M.C. Garner, K.A. Hanold and K.M. Strong, *SPIE Conference on Laser Techniques for State-Selected and State-to-State Chemistry III*, Vol. 2548 (1995) 122.
- [29] R.E. Continetti, D.R. Cyr, D.L. Osborn, D.J. Leahy and D.M. Neumark, *J. Chem. Phys.* 99 (1993) 2616.
- [30] K.A. Hanold, C.R. Sherwood, M.C. Garner and R.E. Continetti, *Rev. Sci. Instrum.*, in press.
- [31] D.J. Lavrich, M.A. Buntine, D. Serxner and M.A. Johnson, *J. Chem. Phys.* 99 (1993) 5910.
- [32] R.N. Zare, *Mol. Photochem.* 4 (1972) 1.
- [33] R.T. Pack, *J. Chem. Phys.* 65 (1976) 4765.
- [34] G. Herzberg, *Molecular spectra and molecular structure*, Vol. III (Van Nostrand Reinhold, New York, 1966) p. 132.
- [35] D. Ray, private communication.